RADIATION EFFECTS ON AN UNSTEADY MHD NATURAL CONVECTIVE FLOW OF A NANOFLUID PAST A VERTICAL PLATE

by

Loganathan PARASURAMAN* *, Nirmal Chand PEDDISETTY, and Ganesan PERIYANNAGOUNDER

Department of Mathematics, Anna University, Chennai, India

Original scientific paper
DOI: 10.2298/TSCI121208155P

Numerical analysis is carried out on an unsteady MHD natural convective boundary layer flow of a nanofluid past an isothermal vertical plate in the presence of thermal radiation. The governing partial differential equations are solved numerically by an efficient, iterative, tri-diagonal, semi-implicit finite-difference method. In particular, the effects of radiation, magnetic field and nanoparticle volume fraction on the flow and heat transfer characteristics are investigated. The nanofluids containing nanoparticles of aluminum oxide, copper, titanium oxide, and silver with nanoparticle volume fraction range less than or equal to 0.04 are considered. The numerical results indicate that in the presence of radiation and magnetic field, an increase in the nanoparticle volume fraction will decrease the velocity boundary layer thickness while increasing the thickness of the thermal boundary layer. Meanwhile, an increase in the magnetic field or nanoparticle volume fraction decreases the average skin-friction at the plate. Excellent validation of the present results has been achieved with the published results in the literature in the absence of the nano-particle volume fraction.

Keywords: *MHD, natural convection, nanofluid, semi-infinite vertical plate, thermal radiation*

Introduction

The study of magnetohydrodynamic (MHD) flow and heat transfer has received considerable attention in recent years due to its wide variety of applications in engineering and technology such as MHD generators, plasma studies, nuclear reactors and geothermal energy extractions. The presence of an external magnetic field is used as a control mechanism in material manufacturing industry, as the convection currents are suppressed by Lorentz force which is produced by the magnetic field. Radiation heat transfer is also essential in many engineering areas as the design of pertinent equipment involves processes occurring at high temperatures. Nuclear power plants, gas turbines and various propulsion devices for aircraft, missiles, satellites, and space vehicles are examples of such engineering areas.

The natural convection heat transfer is a vital phenomenon in the cooling mechanism of various engineering systems due to its minimum cost, low noise, smaller size and reliability. Ostrach [1] reviewed various industrial and engineering applications of natural convection such

* Corresponding author; e-mail: logu@annauniv.edu, nirmalprasad2000@gmail.com

as thermal insulators for buildings, the electronics industry, solar collectors, and cooling systems for nuclear reactors. The study of MHD free convection through a viscous fluid past a semi-infinite vertical plate is considered very essential to understand the behavior of the performance of fluid motion in several applications. The problem of natural convection in a regular fluid past a vertical plate is a classical problem first studied theoretically by Pohlhausen [1]. The similarity solution to this problem was given by Ostrach [2]. Siegel [3] was the first to study the transient free-convective flow past a semi-infinite vertical plate by integral method. Gebhart [4] have studied this problem by an approximate method. Hellums and Churchill [5] employed an explicit finite difference technique, which is conditionally stable and convergent. Takhar *et al.* [6] have considered transient free convection past a semi-infinite vertical plate with variable surface temperature. Soundalgekar and Ganesan [7] have studied transient free convection for the isothermal plate by an implicit finite difference method which is unconditionally stable and convergent.

Convective flows with radiation are also encountered in many industrial processes such as heating and cooling of chambers, energy processes, evaporation from large reservoirs, solar power technology and space vehicle reentry. Thermal radiation effects of an optical thin gray gas bounded by a stationary vertical plate are investigated by England and Emery [8]. Soundalgekar and Takhar [9] have studied the radiation free convective flow of an optically thin gray gas past a semi-infinite vertical plate. Hossain and Takhar [10] have considered the radiation effects on mixed convection along an isothermal vertical plate. Das *et al.* [11] analyzed radiation effects on flow past an impulsively started infinite vertical plate.

Fluid cooling and heating plays an important role in many industries and engineering applications particularly in nuclear reactors, thin film solar energy collectors, manufacturing, power generation and transportation. In these applications use of common heat transfer fluids such as water, ethylene glycol and engine oil limits the heat transfer capabilities due to their poor heat transfer properties. The low thermal conductivity of the conventional heat transfer fluids is a primary limitation in enhancing the performance and the compactness of many engineering electronic devices. Nanofluid is the nanotechnology based heat transfer fluid that can be derived by stably suspending nanometer-sized particles in conventional heat transfer fluids. Nanofluid is the term first coined by Choi [12] to describe this new class of nanotechnology based fluids that exhibit thermal properties superior to those of their host fluids. Nanofluids were found to be devoid of problems such as sedimentation, erosion and high pressure drop due to the small size of the particles and small volume fraction of particles needed to heat transfer enhancement as compared with micro particle slurries. The nanoparticles used in nanofluids are made of metals (Al, Cu), carbides, metal oxides, nitrides or non-metals (graphite, carbon nanotubes) and the base fluid is usually liquid such as water or ethylene glycol.

A comprehensive survey of convective transport in nanofluids was made by Buongiorno [13] who had considered seven slip mechanisms that can produce relative velocity between the nanoparticles and the base fluid. He showed that Brownian diffusion and thermophoresis are important mechanisms in laminar flow. Kuznetsov and Nield [14] investigated the natural convective boundary layer flow of a nanofluid past an infinite vertical plate by considering thermophoresis and Brownian motion of nanoparticles. Nield and Kuznetsov [15] also have studied Cheng-Minkowycz problem for natural convection boundary layer flow in a porous medium saturated by nanofluids. Khan and Pop [16] reported the boundary layer flow of nanofluid past a stretching sheet. The mixed convection MHD flow of a nanofluid over a stretching sheet with the effects of viscous dissipation and variable magnetic field is analyzed by Habibimatin *et al.* [17]. Hamad *et al.* [18] investigated the magnetic field effects on the free

convection flow of a nanofluid past a semi-infinite vertical flat plate. Steady MHD free convective flow of a nanofluid past a vertical plate is investigated by Chamkha and Aly [19]. Entropy analysis for MHD flow over a nonlinear stretching inclined transparent plate embedded in a porous medium due to solar radiation is investigated by Dehsara *et al.* [20]. MHD mixed convective boundary layer flow of a nanofluid through a porous medium due to an exponential stretching sheet is investigated by Ferdows *et al*. [21]. Ahmed *et al.* [22] studied numerically the mixed convection boundary layer flow from a vertical flat plate embedded in a porous medium filled with nanofluids. Hady *et al.* [23] have analyzed the radiation effects on viscous flow of a nanofluid and heat transfer over a non-linearly stretching sheet. Shakhaoath khan *et al.* [24] investigated the effects of magnetic field on radiative flow of a nanofluid past a stretching sheet. Recently, Loganathan *et al.* [25] have reported radiation effects on an unsteady natural convective flow of a nanofluid past an infinite vertical plate.

To authors' knowledge, no studies have been communicated so far with regard to on an unsteady MHD natural convective flow of a nanofluid past an isothermal semi-infinite vertical plate in the presence of radiation. The objective of this paper is to analyze the effects of radiation, magnetic field and nanoparticle volume fraction on transient natural convective flow of Al_2O_3, Cu, TiO_2 and Ag water nanofluids past a semi-infinite vertical plate. The present study is of immediate application to all those processes which are highly affected by heat enhancement concept and magnetic field. The results are validated against nanoparticle volume fraction $\varphi = 0$ and are shown graphically.

Mathematical analysis

A 2-D flow of a viscous incompressible nanofluid past a semi infinite vertical plate is considered. Initially the plate and the fluid are at the same temperature T_∞. Then at time $t' \geq 0$ the temperature of the plate is suddenly raised to T_w and is maintained at the same value. We also assume that x-co-ordinate to be directed upward along the plate and y-co-ordinate is taken normal to the plate. The fluid is water based nanofluid containing different types of nanoparticles: aluminum oxide (Al_2O_3), copper (Cu), titanium oxide (TiO_2), and silver (Ag). In this study, nanofluids are assumed to behave as single phase fluids with local thermal equilibrium between the base fluid and the nanoparticles suspended in them so that no slip occurs between them. A schematic representation of physical model and coordinate system is depicted in fig. 1. The thermo-physical properties of the nanoparticles (ref. [26]) are given in tab. 1. The basic unsteady momentum and thermal energy equations according to the model for nanofluids given by Tiwari and Das [27] satisfying Boussinesq approximation (Schlichting [28]) in the presence of radiation and magnetic field are as follows:

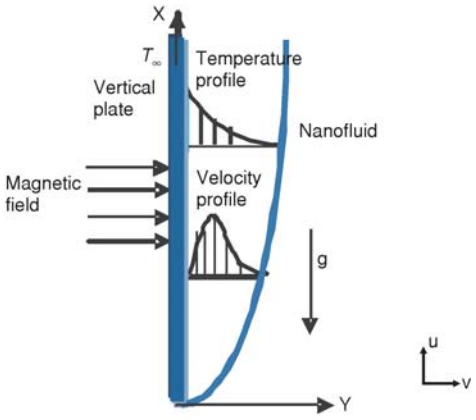

Figure 1. Physical model and coordinate system

$$\frac{\partial u}{\partial x} + \frac{\partial v}{\partial y} = 0 \tag{1}$$

$$\frac{\partial T}{\partial t'} + u\frac{\partial T}{\partial x} + v\frac{\partial T}{\partial y} = \frac{1}{(\rho c_p)_{\mathrm{nf}}}\left[k_{\mathrm{nf}}\frac{\partial^2 T}{\partial y^2} - \frac{\partial q_{\mathrm{r}}}{\partial y}\right] \tag{2}$$

$$\frac{\partial u}{\partial t'} + u\frac{\partial u}{\partial x} + v\frac{\partial u}{\partial y} = \upsilon_{\mathrm{nf}}\frac{\partial^2 u}{\partial y^2} + \frac{(\rho\beta)_{\mathrm{nf}}}{\rho_{\mathrm{nf}}}g(T - T_\infty) - \frac{\sigma B_0^2 u}{\rho_{\mathrm{nf}}} \tag{3}$$

The initial and boundary conditions are:

$$\begin{aligned} &t' \le 0, \quad u = 0, \quad v = 0, \quad T = T_\infty \quad \text{for all} \quad x \text{ and } y \\ &t' > 0, \quad u = 0, \quad v = 0, \quad T = T_\infty \quad \text{at} \quad x = 0 \\ &\qquad\quad u = 0, \quad v = 0, \quad T = T_{\mathrm{w}} \quad \text{at} \quad y = 0 \\ &\qquad\quad u \to 0, \quad v \to 0, \quad T = T_\infty \quad \text{as} \quad y \to \infty \end{aligned} \tag{4}$$

Table 1. Thermo-physical properties of water and nanoparticles

	ρ[kgm^{-3}]	C_p [Jkg^{-1}K^{-1}]	k [Wm^{-1}K^{-1}]	$\beta\cdot10^{-5}$ [K^{-1}]
H_2O	997.1	4179	0.613	21
Al_2O_3	3970	765	40	0.85
Cu	8933	385	401	1.67
TiO_2	4250	686.2	8.9528	0.9
Ag	10500	235	429	1.89

Here u and v are the velocity components in the x- and y--directions; t' is the time; g – the acceleration due to gravity; T – the temperature of the fluid; T_∞ – the temperature of the fluid far away from the plate; T_{w} – the temperature of the plate; q_{r} – the radiative heat flux, and B_0 – the strength of applied magnetic field. For nanofluids the expressions of density ρ_{nf}, thermal expansion coefficient $(\rho c_p)_{\mathrm{nf}}$ and heat capacitance $(\rho c_p)_{\mathrm{nf}}$ are given by:

$$\begin{aligned} \rho_{\mathrm{nf}} &= (1-\varphi)\rho_{\mathrm{f}} + \varphi\rho_{\mathrm{s}} \\ (\rho\beta)_{\mathrm{nf}} &= (1-\varphi)(\rho\beta)_{\mathrm{f}} + \varphi(\rho\beta)_{\mathrm{s}} \\ (\rho c_p)_{\mathrm{nf}} &= (1-\varphi)(\rho c_p)_{\mathrm{f}} + \varphi(\rho c_p)_{\mathrm{s}} \end{aligned} \tag{5}$$

The effective thermal conductivity of the nanofluid according to Hamilton and Crosser model [29] is given by:

$$\frac{k_{\mathrm{eff}}}{k_{\mathrm{f}}} = \frac{k_{\mathrm{s}} + (n-1)k_{\mathrm{f}} - (n-1)\varphi(k_{\mathrm{f}} - k_{\mathrm{s}})}{k_{\mathrm{s}} + (n-1)k_{\mathrm{f}} + \varphi(k_{\mathrm{f}} - k_{\mathrm{s}})} \tag{6}$$

where n is the empirical shape factor for the nanoparticle. In particular, $n = 3$, for spherical shaped nanoparticles and $n = 3/2$ for cylindrical ones. φ is the solid volume fraction of nanoparticles, μ – the dynamic viscosity, υ – the kinematic viscosity, β – the thermal expansion coefficient, ρ – the density, and k – the thermal conductivity. Here the subscripts nf, f, and s represent the thermo-physical properties of the nanofluids, base fluid, and the solid nanoparticles, respectively.

Assuming the Rosseland approximation [30], leads to the radiative heat flux:

$$q_{\mathrm{r}} = \frac{4\sigma^*}{3k^*}\frac{\partial T^4}{\partial y} \tag{7}$$

where σ^* and k^* are Stefan-Boltzmann constant and the mean absorption coefficient.

$$\frac{\partial q_{\mathrm{r}}}{\partial y} = -4a^*\sigma^*(T_\infty^4 - T^4) \tag{8}$$

If the temperature differences within the flow are sufficiently small such that T^4 may be expressed as a linear function of temperature, then expanding T^4 in Taylor series about T_∞ and neglecting higher order terms, we get:

$$T^4 \cong 4T_\infty^3 T - 3T_\infty^4 \tag{9}$$

We now introduce the following non-dimensional quantities in eqs. (1) to (3):

$$X = \frac{x}{L},\ Y = \frac{y\sqrt[4]{\mathrm{Gr}}}{L},\ U = \frac{uL\mathrm{Gr}^{-1/2}}{\upsilon_f},\ V = \frac{v\mathrm{Gr}^{-1/4}}{\upsilon_\mathrm{f}},\ t = \frac{t'\upsilon_\mathrm{f}\sqrt{\mathrm{Gr}}}{L^2},\ \theta = \frac{T - T_\infty}{T_\mathrm{w} - T_\infty},$$

$$\mathrm{Pr} = \frac{\upsilon_\mathrm{f}}{\alpha_\mathrm{f}},\ \mathrm{Gr} = \frac{g\beta L^3 (T_\mathrm{w} - T_\infty)}{\upsilon_f^2},\ M = \frac{\sigma B_0^2 L^2}{\mu_\mathrm{f}\sqrt{\mathrm{Gr}}},\ \text{and}\ R = \frac{16a^*\sigma T_\infty^3 L^2 \mathrm{Gr}^{-1/2}}{k_\mathrm{f}} \tag{10}$$

where Gr is the Grashof number and Pr is the Prandtl number.

Now eqs. (1) to (3) in view of the eqs. (5) to (9) are:

$$\frac{\partial U}{\partial X} + \frac{\partial V}{\partial Y} = 0 \tag{11}$$

$$\frac{\partial \theta}{\partial t} + U\frac{\partial \theta}{\partial X} + V\frac{\partial \theta}{\partial Y} = \frac{1}{\left[1 - \varphi + \varphi\dfrac{(\rho c_p)_\mathrm{s}}{(\rho c_p)_\mathrm{f}}\right]}\left(\frac{k_\mathrm{nf}}{k_\mathrm{f}}\frac{1}{\mathrm{Pr}}\frac{\partial^2\theta}{\partial Y^2} - \frac{R\theta}{\mathrm{Pr}}\right) \tag{12}$$

$$\frac{\partial U}{\partial t} + U\frac{\partial U}{\partial X} + V\frac{\partial U}{\partial Y} = \frac{1}{1 - \varphi + \varphi\dfrac{\rho_\mathrm{s}}{\rho_\mathrm{f}}}\left[\frac{1}{(1-\varphi)^{2.5}}\frac{\partial^2 U}{\partial Y^2} + \left(1 - \varphi + \varphi\frac{(\rho\beta)_\mathrm{s}}{(\rho\beta)_\mathrm{f}}\right)\theta - MU\right] \tag{13}$$

The transformed boundary conditions are:

$$\begin{aligned}
&t \le 0,\ U = 0,\ V = 0,\ \theta = 0 \quad \text{for all} \quad X \text{ and } Y\\
&t > 0,\ U = 0,\ V = 0,\ \theta = 0 \quad \text{at} \quad X = 0\\
&\qquad U = 0,\ V = 0,\ \theta = 1 \quad \text{at} \quad Y = 0\\
&\qquad U \to 0,\ V \to 0,\ \theta \to 0 \quad \text{as} \quad Y \to \infty
\end{aligned} \tag{14}$$

Let

$$E_1 = \frac{k_{nf}}{k_f}\frac{1}{\mathrm{Pr}}\left(\frac{1}{1 - \varphi + \varphi\dfrac{(\rho c_p)_\mathrm{s}}{(\rho c_p)_\mathrm{f}}}\right),\quad E_2 = \frac{1}{(1-\varphi)^{2.5}}\left(\frac{1}{1 - \varphi + \varphi\dfrac{\rho_\mathrm{s}}{\rho_\mathrm{f}}}\right),$$

$$E_3 = \frac{1 - \varphi + \varphi\dfrac{(\rho\beta)_\mathrm{s}}{(\rho\beta)_\mathrm{f}}}{1 - \varphi + \varphi\dfrac{\rho_\mathrm{s}}{\rho_\mathrm{f}}},\quad E_4 = \frac{1}{1 - \varphi + \varphi\dfrac{\rho_\mathrm{s}}{\rho_\mathrm{f}}},\quad E_5 = \frac{1}{1 - \varphi + \varphi\dfrac{(\rho c_p)_\mathrm{s}}{(\rho c_p)_\mathrm{f}}} \tag{15}$$

Table 2. Thermal conductivity and dynamic viscosity for various shapes of nanoparticles

Model	Shape of nanoparticles	Thermal conductivity	Dynamic viscosity
I	Spherical	$\frac{k_{nf}}{k_f}=\frac{k_s+2k_f-2\varphi(k_f-k_s)}{k_s+2k_f+\varphi(k_f-k_s)}$	$\mu_{nf}=\frac{\mu_f}{(1-\varphi)^{2.5}}$
II	Spherical	$\frac{k_{nf}}{k_f}=\frac{k_s+2k_f-2\varphi(k_f-k_s)}{k_s+2k_f+\varphi(k_f-k_s)}$	$\mu_{nf}=\mu_f(1+7.3\varphi+123\varphi^2)$
III	Cylindrical (nano tubes)	$\frac{k_{nf}}{k_f}=\frac{k_s+\frac{1}{2}k_f-\frac{1}{2}\varphi(k_f-k_s)}{k_s+\frac{1}{2}k_f+\varphi(k_f-k_s)}$	$\mu_{nf}=\frac{\mu_f}{(1-\varphi)^{2.5}}$
IV	Cylindrical (nano tubes)	$\frac{k_{nf}}{k_f}=\frac{k_s+\frac{1}{2}k_f-\frac{1}{2}\varphi(k_f-k_s)}{k_s+\frac{1}{2}k_f+\varphi(k_f-k_s)}$	$\mu_{nf}=\mu_f(1+7.3\varphi+123\varphi^2)$

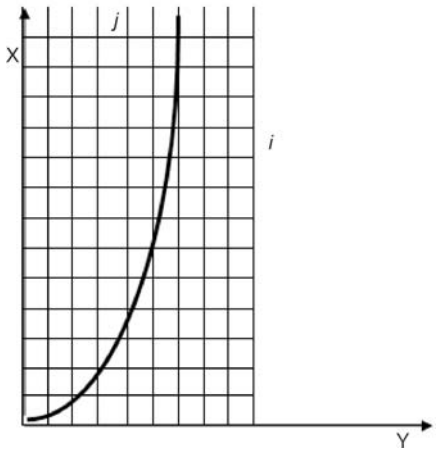

Figure 2. Discretization of domain

Numerical procedure

The set of two-dimensional, coupled, non-linear partial differential equations (11)-(13) under the initial and boundary conditions (14) is solved using a semi-implicit finite difference method. So we express them by finite-difference scheme of Crank-Nicolson type, which converges faster and also stable unconditionally [31]. The region of integration is considered as a rectangle as shown in fig. 2 .The finite difference equations at every internal nodal point for a particular *i*-level constitute a tri-diagonal system, which is solved by applying Thomas algorithm. Computations are carried out for all the time levels until the steady--state is reached. The steady-state solution is assumed to have been reached, when the absolute difference between the values of U, as well as temperature T at two consecutive time steps are less than 10^{-5} at all grid points.

The temperatures at two time levels are shown in the tab. 3. The steady-state is reached at $t = 9.15002$ when the absolute difference between temperatures is less than 10^{-5}.

Table 3. Comparison of temperatures at two different time levels

		Y	0	0.5	1	1.5	2	2.5	3	3.5	4	4.5
Time	9.15002	T1	1	0.77543	0.44825	0.24403	0.12592	0.06245	0.0301	0.01416	0.00649	0.00287
Time	9.10002	T2	1	0.77543	0.44825	0.24403	0.12592	0.06244	0.03009	0.01415	0.00648	0.00286
Δt	0.05	T1-T2	0	0	0	0	0	1E-05	1E-05	1E-05	1E-05	0.00001

Stability and convergence of the finite difference scheme

The finite difference equations corresponding to U and θ are:

$$\frac{U_{i,j}^{n+1}-U_{i,j}^{n}}{\Delta t}+U_{i,j}^{n}\frac{U_{i,j}^{n+1}-U_{i-1,j}^{n+1}+U_{i,j}^{n}-U_{i-1,j}^{n}}{2\Delta X}+V_{i,j}^{n}\frac{U_{i,j+1}^{n+1}-U_{i,j-1}^{n+1}+U_{i,j+1}^{n}-U_{i,j-1}^{n}}{4\Delta Y}=$$
$$=E_2\left(\frac{U_{i,j-1}^{n+1}-2U_{i,j}^{n+1}+U_{i,j+1}^{n+1}+U_{i,j-1}^{n}-2U_{i,j}^{n}+U_{i,j+1}^{n}}{2(\Delta Y)^2}\right)+$$
$$+E_3\left(\frac{\theta_{i,j}^{n+1}+\theta_{i,j}^{n}}{2}\right)-ME_4\left(\frac{U_{i,j}^{n+1}+U_{i,j}^{n}}{2}\right) \tag{16}$$

$$\frac{\theta_{i,j}^{n+1}-\theta_{i,j}^{n}}{\Delta t}+U_{i,j}^{n}\left(\frac{\theta_{i,j}^{n+1}-\theta_{i-1,j}^{n+1}+\theta_{i,j}^{n}-\theta_{i-1,j}^{n}}{2\Delta X}\right)+V_{i,j}^{n}\left(\frac{\theta_{i,j+1}^{n+1}-\theta_{i,j-1}^{n+1}+\theta_{i,j+1}^{n}-\theta_{i,j-1}^{n}}{4\Delta Y}\right)=$$
$$=E_1\left(\frac{\theta_{i,j-1}^{n+1}-2\theta_{i,j}^{n+1}+\theta_{i,j+1}^{n+1}+\theta_{i,j-1}^{n}-2\theta_{i,j}^{n}+\theta_{i,j+1}^{n}}{2(\Delta Y)^2}\right)-E_5\frac{R}{\mathrm{Pr}}\left(\frac{\theta_{i,j}^{n+1}+\theta_{i,j}^{n}}{2}\right) \tag{17}$$

The stability criterion of the scheme for constant mesh sizes is proved as: The general term of the Fourier expansion for U, θ at time $t = 0$ are all $e^{i\alpha X}e^{i\beta Y}$ apart from a constant $i = (-1)^{1/2}$. At a later time t, these terms will become:

$$U=\psi(t)e^{i\alpha X}e^{i\beta Y} \tag{18}$$

$$\theta=\Phi(t)e^{i\alpha X}e^{i\beta Y} \tag{19}$$

Substituting U and θ in eqs. (20) and (21), regarding the coefficients U and V as constants over any one time step and denoting the values after a time step by ψ', and Φ':

$$\frac{\psi'-\psi}{\Delta t}+\frac{U}{2}\frac{(\psi'-\psi)(1-e^{i\alpha\Delta X})}{\Delta X}+\frac{V}{4}\frac{(\psi'-\psi)(2i\sin\beta\Delta Y)}{\Delta Y}=$$
$$=E_2\frac{(\psi'-\psi)(\cos\beta\Delta-1)}{(\Delta Y)^2}+\frac{E_3}{2}(\Phi'+\Phi)-\frac{ME_4}{2}(\psi'-\psi) \tag{20}$$

$$\frac{\Phi'-\Phi}{\Delta t}+\frac{U}{2}\frac{(\Phi'+\Phi)(1-e^{i\alpha\Delta X})}{\Delta X}+\frac{V}{4}\frac{(\Phi'+\Phi)(2i\sin\beta\Delta Y)}{\Delta}=E_1\frac{(\Phi'+\Phi)(\cos\beta\Delta Y-1)}{(\Delta Y)^2} \tag{21}$$

Let

$$A=\frac{U}{2}\frac{\Delta t}{\Delta X}(1-e^{-i\alpha\Delta X})+\frac{V}{2}\frac{\Delta t}{\Delta Y}(i\sin\beta\Delta Y)-E_2\frac{\Delta t}{(\Delta Y)^2}(\cos\beta\Delta Y-1)+E_4\frac{M}{2}\Delta t \tag{22}$$

$$B=\frac{U}{2}\frac{\Delta t}{\Delta X}(1-e^{-i\alpha\Delta X})+\frac{V}{2}\frac{\Delta t}{\Delta Y}(i\sin\beta\Delta Y)-E_1\frac{\Delta t}{(\Delta Y)^2}(\cos\beta\Delta Y-1)+E_5\frac{R}{\mathrm{Pr}}\Delta t \tag{23}$$

Substituting A and B in eqs. (25) and (26), we have:

$$(1+A)\psi'=(1-A)\psi+E_3\frac{\Delta t}{2}(\Phi'+\Phi) \tag{24}$$

$$(1+B)\Phi'=(1-B)\Phi \tag{25}$$

Equations (24) and (25) can be written in the matrix form:

$$\begin{bmatrix}\psi'\\ \Phi'\end{bmatrix}=\begin{bmatrix}\dfrac{1-A}{1+A} & \dfrac{E_3\Delta t}{(1+A)(1+B)}\\ 0 & \dfrac{1-B}{1+B}\end{bmatrix}\begin{bmatrix}\psi\\ \Phi\end{bmatrix},\quad \eta'=E\eta \tag{26}$$

where η is a column vector of elements ψ and Φ.

Now, for stability the modulus of each eigenvalue of the amplification matrix E should not exceed unity.

The eigenvalues of E are: $(1 - A)/(1 - A)$ and $(1 + B)/(1 + B)$.

Assume that U is everywhere positive and V is everywhere negative and let:

$$a=\frac{U}{2}\frac{\Delta t}{\Delta X},\quad b=\frac{|V|}{2}\frac{\Delta t}{\Delta X},\quad c=\frac{\Delta t}{(\Delta Y)^2},\quad d=\Delta t$$

Substituting in eq. (27), we have:

$$A=2a\sin^2\frac{\alpha\Delta X}{2}+2c\sin^2\frac{\beta\Delta Y}{2}+i(a\sin\alpha\Delta X-b\sin\beta\Delta Y)+E_4\frac{M}{2}d$$

Since the real part of A is greater than or equal to zero, we have $|(1 - A)/(1 + A)| \le 1$. Similarly, $|(1 - B)/(1 + B)| \le 1$.

Hence the scheme is unconditionally stable which is also shown by Soundalgekar and Ganesan [7] for ordinary fluids. The local truncation error is $o(\Delta t^2 + DX + \Delta Y^2)$ and it tends to zero as Δt, ΔX, and ΔY tend to zero. Hence the scheme is compatible. The stability and compatibility ensures the convergence of the finite difference scheme.

Nusselt number

The local as well as average values of Nusselt number in dimensionless form are:

$$\mathrm{Nu}_X=\frac{-k_{nf}}{k_f}X\sqrt[4]{\mathrm{Gr}}\left(\frac{\partial\theta}{\partial Y}\right)_{Y=0} \tag{27}$$

$$\mathrm{Nu}=\frac{-k_{nf}}{k_f}\sqrt[4]{\mathrm{Gr}}\int_0^1\left(\frac{\partial\theta}{\partial Y}\right)_{Y=0}\mathrm{d}X \tag{28}$$

The derivatives involved in eqs. (27) and (28) are evaluated by using a five-point approximation formula and the integrals are evaluated by Newton-Cotes closed integration formula.

Results and discussion

In order to get the physical insight into the flow problem, numerical computations are carried out for various values of parameters that describe the flow characteristics and the results are illustrated graphically. The dimensionless partial differential equations together with the appropriate boundary conditions are solved by a semi-implicit finite-difference method of Crank Nicolson type. The step size $\eta = 0.05$ is used to obtain the numerical solution. We consider four different types of nanofluids containing aluminum oxide, titanium oxide, copper, and silver nanoparticles with water as a base fluid. The nanoparticle volume fraction is considered in the range of $0 \le \varphi \le 0.04$, as sedimentation takes place when the nanoparticle volume fraction exceeds 8%. In this study, we have considered spherical nanoparticles with thermal conductivity and dynamic viscosity shown in Model I in tab. 2. The Prandtl number, of the base fluid is kept constant at 6.2. The effects of nanoparticle volume fraction, magnetic field, and radiation on the

transient velocity and temperature profiles of the nanofluids are plotted. When $\varphi = 0$ this study reduces the governing equations to those of a regular fluid. In order to verify the accuracy of the numerical method, the present results are compared with those of Takhar *et al.* [6] in the literature and the comparisons are in excellent agreement as shown in fig. 3.

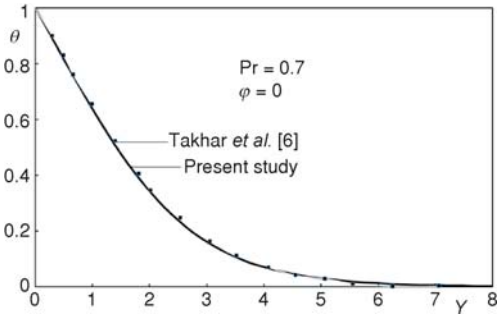

Figure 3. Comparison of temperature profiles of Cu water nanofluid with Takhar *et al.* [6]

Figure 4 depicts the velocity profiles of copper water nanofluid for different values of magnetic and radiation parameters. The velocity of the copper water nanofluid decreases with an increase in magnetic field and radiation. The applied magnetic field has the tendency to slow down the movement of the fluid as a result of increased retarding force. Hence, the presence of a magnetic field decreases the momentum boundary layer thickness. This causes the velocity profiles of the nanofluid to have distinctive peaks near the immediate vicinity of the plate and as M increases these peaks decrease and move gradually downstream. In addition, this decrease in the flow movement is also accompanied by an increase in the radiation parameter.

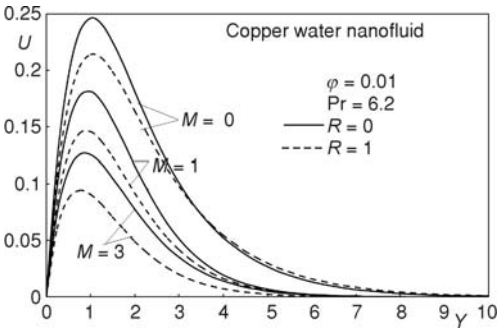

Figure 4. Comparison of velocity profiles of Cu water nanofluid for different values of *M* and *R*

Figure 5 illustrates the velocity profiles of copper water nanofluid for various values of the nanoparticle volume fraction in simultaneous absence and presence of radiation and magnetic fields. It is observed that in the presence of radiation and magnetic fields, the velocity of the nanofluid increases with nanoparticle volume fraction, whereas, the converse is true in the absence of radiation and magnetic fields.

Figure 6 shows the velocity profiles of silver water nanofluid in the presence of radiation and magnetic field with respect to time. It is observed that the velocity of the nanofluid increases with respect to time and a steady-state is reached when $t = 9.2$. The velocity of the nanofluid reaches a temporal maximum, which is observed at $t = 6.05$.

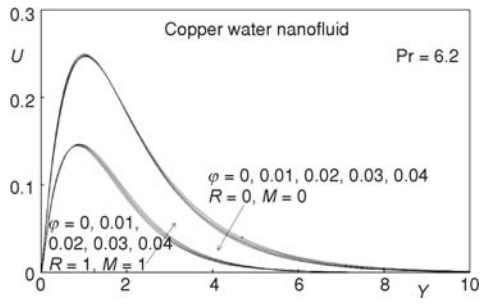

Figure 5. Velocity profiles of Cu water nanofluid for different values of *M* and *R*

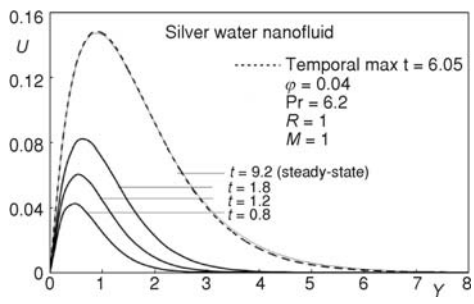

Figure 6. Transient velocity profiles of Ag water nanofluid

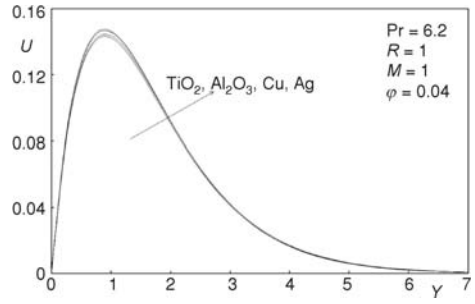

Figure 7. Velocity profiles of various nanofluids

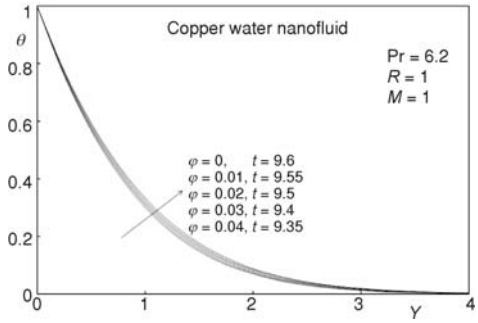

Figure 9. Temperature profiles of Cu water nanofluid for different values of φ

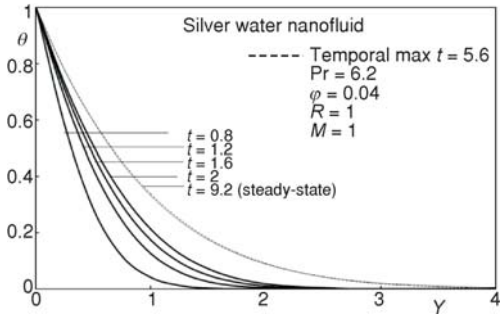

Figure 10. Transient temperature profiles of Ag water nanofluid

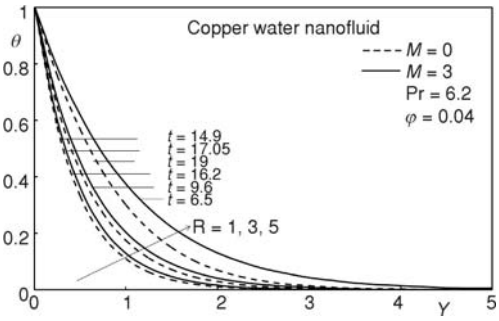

Figure 8. Transient temperature profiles of Cu water nanofluid for different values of *M* and *R*

It is observed from fig. 8 that the temperature profiles of copper water nanofluid increases in the presence of both magnetic field and radiation. Radiation increases the rate of energy transport to the fluid and hence the thermal boundary layer thickness increases. The effect of a transverse magnetic field on the fluid give rise to a resistive type force called the Lorentz force. This force has the tendency to slow down the motion of the fluid to increase the temperature boundary layer. The presence of a magnetic field increases the temperature inside the boundary layer as shown in fig. 8.

The steady-state temperature profiles of copper water nanofluid with respect to the nanoparticle volume fraction φ are shown in fig. 9. As the nanoparticle volume fraction increases the temperature of the nanofluid decreases in the presence of radiation and magnetic parameter. This is possible physically because an increase in the nanoparticle volume fraction leads to an increase in the thermal conductivity of the nanofluid and hence the thickness of the thermal boundary layer increases. The time taken to reach steady state decreases with an increase in nanoparticle volume fraction φ.

The temperature profiles of silver water nanofluid increases with time when $R = 1$ and $M = 1$. The temporal maximum for silver water nanofluid is observed at time $t = 5.6$ and steady-state is reached at $t = 9.2$ as shown in fig. 10.

Computations of local Nusselt number for various nanofluids are shown in the tab. 3. The effects of thermal radiation and magnetic field on a local Nusselt number of silver water nanofluid are depicted in fig. 11. It is observed that local Nusselt number increases with an increase in the thermal radiation parameter. The magnetic field retards the heat transfer process by

decreasing the local Nusselt number. Enhancing magnetic field tends to decrease the fluid velocity and hence decrease the local Nusselt number.

Table 4. Local Nusselt number of various nanofluids in the presence of magnetic field and radiation

Pr = 6.2, R = 1, M = 1, φ = 0.04										
X	0.5	1	1.5	2	2.5	3	3.5	4	4.5	5
Ag	0.1360	0.2179	0.2994	0.3788	0.4567	0.5337	0.6100	0.6860	0.7616	0.8371
Cu	0.1356	0.2172	0.2985	0.3776	0.4552	0.5319	0.6081	0.6838	0.7592	0.8344
Al_2O_3	0.1365	0.2187	0.3006	0.3803	0.4585	0.5357	0.6123	0.6885	0.7643	0.8400
TiO_2	0.1372	0.2197	0.3020	0.3821	0.4608	0.5386	0.6158	0.6925	0.7691	0.8454

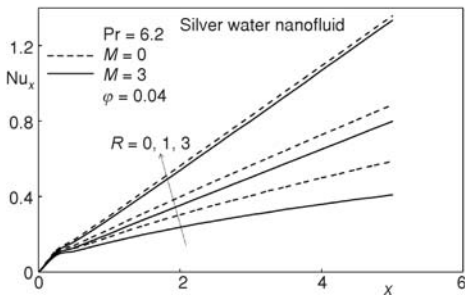

Figure 11. Local Nusselt number of Ag water nanofluid for different values of *R* & *M*

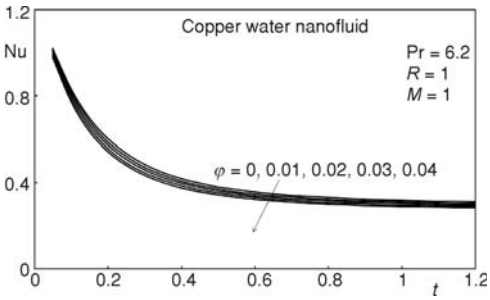

Figure 12. Average Nusselt number of Cu water nanofluid

Figure 12 illustrates that the average Nusselt number of copper water nanofluid decreases with an increase in the nanoparticle volume fraction when R = 1 and M = 1. This concludes that changes in heat transfer rates are associated with nanoparticle volume fraction, which indicates the possible use of nanofluids in heat transfer processes.

From fig. 13 it is observed that the presence of a magnetic field and radiation decreases the heat transfer rates of nanofluids. Figure 14 shows that an increase in radiation parameter increases the local skin friction (τ_x) in the absence of magnetic field and in the presence of mag-

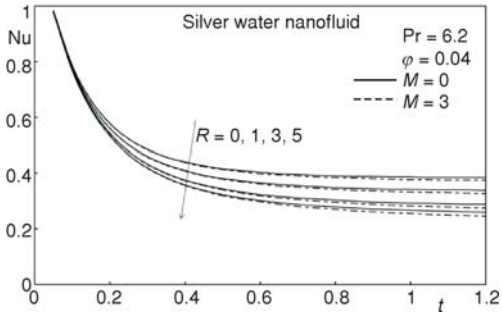

Figure 13. Average Nusselt number of Ag water nanofluid for different values of *R* & *M*

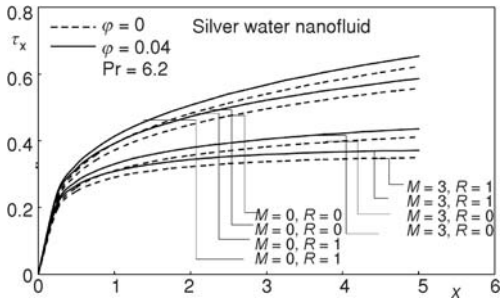

Figure 14. Local skin-friction of Ag water nanofluid and water for different values of *M* and *R*

netic field an increase in radiation decreases the local skin friction. It is also observed that an increase in the nanoparticle volume fraction increases the local skin friction.

Figure 15 shows that an increase in the nanoparticle volume fraction decreases the average skin-friction in the presence of radiation and magnetic field. This suggests that the presence of nanoparticles decreases the average skin-friction when the radiation and magnetic fields are present.

Figure 16 concludes that an increase in radiation and magnetic field decreases the average skin-friction of silver water nanofluid. Thus the presence of the magnetic field helps in reducing the frictional drag on the surface and an increase in the radiation parameter tends to reduce the velocity as shown in fig. 4.

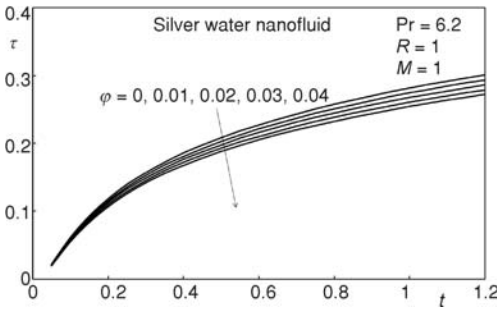

Figure 15. Average nanoparticle volume fraction of Ag water nanofluid for different values of *R* & *M*

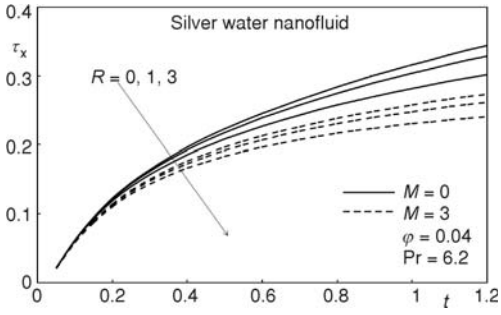

Figure 16. Concludes that an increase in radiation and magnetic field decreases the local skin-friction of Ag water nanofluid

Conclusions

In this paper, the problem of radiation effects on an unsteady MHD flow of a nanofluid past a semi-infinite vertical plate is considered. The effects of radiation, magnetic parameter and a nanoparticle volume fraction of the flow and heat transfer characteristics are determined for four kinds of nanofluids: aluminum oxide, copper, titanium oxide, and silver. The dimensionless partial differential equations with the appropriate boundary conditions are solved numerically by an implicit finite difference method which is unconditionally stable and convergent. The conclusions of this study are as follows.

- In the presence of radiation and magnetic field, an increase in nanoparticle volume fraction φ decreases the nanofluid temperature, which leads to a decrease in the heat transfer rates.
- Increase in nanoparticle volume fraction increases the dimensionless surface velocity of the fluid in the presence of magnetic field and radiation, which in turn decreases the average skin-friction.
- The presence of radiation and magnetic field increases the temperature of the nanofluid with time.
- The rate of heat transfer at the plate decreases with an increase in the radiation and magnetic field.
- The velocity of the nanofluid decreases with an increase in the radiation and magnetic field, whereas, the temperature of the nanofluid increases.
- The presence of radiation and magnetic field increases transient velocity and temperature profiles of nanofluid. They reach a steady state and temporal maximum is observed in each case.

- The average Nusselt number is independent of time when it is large and decreases sharply for smaller values of *t*.
- Time required reaching the steady-state decreases with an increase in the nanoparticle volume fraction.
- Average skin-friction increases for smaller values of *t*.

The unsteady MHD natural convective flow of nanofluids past a semi-infinite vertical plate has immediate applications in all those processes which are highly affected by heat transfer concept. One of the technological applications of nanoparticles is the use of heat transfer fluids containing suspensions of nanoparticles to confront cooling problems in the thermal systems.

Acknowledgment

The authors wish to express their sincere thanks to the reviewers for their valuable comments and suggestions, which have led to definite improvement in the paper.

References

[1] Pohlhausen, E., The Heat Exchange between Solid Body and Fluid with Small Friction and Low Heat Transfer (in German), *Z. Angew. Math. Mech., 1* (1921), pp. 115-121
[2] Ostrach, S., An Analysis of Laminar Free-Convection Flow and Heat Transfer about a Flat Plate Parallel to the Direction of the Generating Body Force, *NACA Annual Report 39-Vol-1, 1111,* 1953, pp. 63-79
[3] Siegel, R., Transient Free Convection From a Vertical Flat Plate, *Transactions of American Society of Mech. Eng., 80* (1958), pp. 347-359
[4] Gebhart, B., Pera, L., The Nature of Vertical Natural Convection Flows Resulting from the Combined Buoyancy Effects of Thermal and Mass Diffusion, *Int. J. Heat Mass Transf., 14* (1971), 12, pp. 2025-2050
[5] Hellums, J. D., Churchill, S.W., Transient and Steady State, Free and Natural Convection, Numerical Solutions, Part 1. The Isothermal Vertical Plate, *American Institute of Chem. Engineers Journal, 8* (1962), 5, pp. 690-692
[6] Takhar, H. S., *et al*., Transient Free Convection Past a semi-infinite vertical plate with Variable Surface Temperature, *Int. J. Numerical Methods for Heat and Fluid Flow, 7* (1996), 4, pp. 280-296
[7] Soundalgekar, V. M., Ganesan, P., The finite Difference Analysis of Transient Free Convection with Mass Transfer of an Isothermal Vertical Flat Plate, *Int. J. Engineering Sciences, 19* (1981), 6, pp. 757-770
[8] England, W. G., Emery, A. F., Thermal Radiation Effects on the Laminar Free Convection Boundary Layer of an Absorbing Gas, *J. Heat Transf., 91* (1969), 1, pp. 37-44
[9] Soundalgekar, V. M., Takhar, H. S., Radiation Effects on Free Convection Flow past a Semi-Infinite Vertical Plate, Modelling, *Measurement and Control, B51* (1993), pp. 31-40
[10] Hossain, M. A., Takhar, H. S., Radiation Effect on Mixed Convection Along a Vertical Plate with Uniform Surface Temperature, *J. Heat and Mass Transf., 31* (1996), 4, pp. 243-248
[11] Das, U. N., *et al.*, Radiation Effects on Flow Past an Impulsively Started Vertical Infinite Plate, *J. Theoretical Mech., 1* (1996), 5, pp. 111-115
[12] Choi, S. U. S., Enhancing Thermal Conductivity of Fluids with Nano- Particles, in: Developments Applications of Non-Newtonian Flows (Eds. D. A. Siginer, H. P. Wang), FED-vol. 231/MD-vol. 66, ASME, New York, 1995, pp. 99-105
[13] Buongiorno, J., Convective Transport in Nanofluids, *J. Heat Transf., 128* (2006), 3, pp. 240- 250
[14] Kuznetsov, A. V., Nield, D. A., Natural Convective Boundary-Layer Flow of a Nanofluid Past a Vertical Plate, *Int. J. Therm. Sci., 49* (2010), 2, pp. 243-247
[15] Nield, D. A., Kuznetsov, A. V., The Cheng-Minkowycz Problem for Natural Convective Boundary-Layer Flow in a Porous Medium Saturated by a Nanofluid, *Int. J. Heat and Mass Transf., 52* (2009), 25-26, pp. 5792-5795
[16] Khan, W. A., Pop, I., Boundary-Layer Flow of a Nanofluid Past a Stretching Sheet, *Int. J. Heat and Mass Transf., 53* (2010), 11-12, pp. 2477-2483
[17] HabibiMatin, M., *et al*., Mixed Convection MHD Flow of Nanofluid over a Non-Linear Stretching Sheet with Effects of Viscous Dissipation and Variable Magnetic Field, *MECHANIKA, 18* (2012), 4, pp. 415-423

[18] Hamad, M. A. A., *et al*., Magnetic Field Effects on Free Convection Flow of a Nanofluid Past a Vertical Semi-Infinite Flat Plate, *Nonlinear Analysis.: Real World Applications, 12* (2011), 3, pp. 1338-1346
[19] Chamkha, A. J., Aly, A. M., MHD Free Convection Flow of a Nanofluid Past a Vertical Plate in the Presence of Heat Generation or Absorption Effects, *Chem. Eng. Comm., 198* (2011), 3, pp. 425-441
[20] Dehsara, M., *et al*., Entropy Analysis for MHD Flow Over a Non-Linear Stretching Inclined Transparent Plate Embedded in a Porous Medium Due to Solar Radiation, *Mechanika, 18* (2012), 5, pp. 524-533
[21] Ferdows, M., *et al.*, MHD Mixed Convective Boundary Layer Flow of a Nanofluid through a Porous Medium Due to an Exponentially Stretching Sheet, *Mathematical problems in Eng., 3* (2012), 7, pp. 2551-1557
[22] Ahmed, S., Pop, I., Mixed Convection Boundary Layer Flow from a Vertical Flat Plate Embedded in a Porous Medium Filled with Nanofluids, *Int. Comm. Heat and Mass Transf., 37* (2010), 8, pp. 987-991
[23] Hady, F. M., *et al*., Radiation Effect on Viscous Flow of a Nanofluid and Heat Transfer over a Nonlinearly Stretching Sheet, *Nanoscale Res. Lett., 7* (2012), 1, pp. 229-241
[24] Shakhaoath Khan, M., *et al*., Effects of Magnetic field on Radiative flow of a Nanofluid Past a Stretching Sheet, *Procedia Engineering, 56* (2013), pp. 316-322
[25] Loganathan, P., *et al.*, Radiation Effects on an Unsteady Natural Convective Flow of a Nanofluid Past an Infinite Vertical Plate, *NANO, 8* (2013), 1, pp. 1350001-1350010
[26] Oztop, H. F., Abu-Nada, E., Numerical Study of Natural Convection in Partially Heated Rectangular Enclosures Filled with Nanofluids, *Int. J. Heat Fluid flow, 29* (2008), pp. 1326-1336
[27] Tiwari, R. K., Das, M. K., Heat Transfer Augmentation in a Two-Sided Lid-Driven Differentially Heated Square Cavity Utilizing Nanofluids, *Int. J. Heat and Mass Transf., 50* (2007), 9-10, pp. 2002-2018
[28] Schlichting, H., Gersten, K., *Boundary Layer Theory*, Springer-Verlag, New York, USA, 2001
[29] Hamilton, R. L., Crosser, O. K., Thermal Conductivity of Heterogeneous Two Component System, *Ind. Eng. Chem. Fundamental, 1* (1962), 3, pp.187-191
[30] Brewster, M. Q., *Thermal Radiative Transfer and Properties*, John Wiley and Sons, New York, USA,1992
[31] Smith, G. D., Numerical Solution of Partial Differential Equations: Finite Difference Methods, Oxford University Press, USA, 1986

Paper submitted: December 8, 2012
Paper revised: September 7, 2013
Paper accepted: November 7, 2013